Novel 8-(furan-2-yl)-3-substituted thiazolo [5,4-*e*][1,2,4] triazolo[1,5-*c*] pyrimidine-2(3*H*)-thione derivatives as potential adenosine A$_{2A}$ receptor antagonists

Chandra Bhushan Mishra, Sandeep Kumar Barodia, Amresh Prakash, J. B. Senthil Kumar, Pratibha Mehta Luthra *

Medicinal Chemistry Division, Dr. B.R. Ambedkar Center for Biomedical Research, University of Delhi, North Campus, Mall Road, Delhi 110 007, India

ABSTRACT

Novel thiazolotriazolopyrimidine derivatives (**23–33**) designed as potential adenosine A$_{2A}$ receptor (A$_{2A}$R) antagonists were synthesized. Molecular docking studies revealed that all compounds (**23–33**) exhibited strong interaction with A$_{2A}$R. The strong interaction of the compounds (**23–33**) with A$_{2A}$R in silico was confirmed by their high binding affinity with human A$_{2A}$R stably expressed in HEK293 cells using radioligand-binding assay. The compounds **24–26** demonstrated substantial binding affinity and selectivity for A$_{2A}$R as compared to SCH58261, a standard A$_{2A}$R antagonist. Decrease in A$_{2A}$R-coupled release of endogenous cAMP in treated HEK293 cells demonstrated in vitro A$_{2A}$R antagonist potential of the compounds **24–26**. Attenuation in haloperidol-induced motor impairments (catalepsy and akinesia) in Swiss albino male mice pre-treated with compounds **24–26** further supports their role in the alleviation of PD symptoms.

© 2010 Elsevier Ltd. All rights reserved.

1. Introduction

Adenosine alters vitally imperative processes in the CNS[1] and is natural ligand at the four well-conserved adenosine receptor subtypes viz. A$_1$, A$_{2A}$, A$_{2B}$ and A$_3$ belonging to G protein coupled receptors.[2] Adenosine A$_{2A}$ receptor (A$_{2A}$R), 45 kDa protein[3] is mainly expressed in the nigrostriatum (basal ganglia) co-localized with dopamine D$_2$ receptors on striatopallidal output neurons.[4] A$_{2A}$Rs are abundantly expressed within striatum in a subset of γ-amino-butyric acid (GABA-ergic) output neurons, which coexpress higher levels of the dopamine D$_2$ receptor and project to the globus pallidus (GP).[5] A$_{2A}$R antagonist activates nigro-striatal pathway via D$_2$ receptor leading to antiparkinsonian effect.[6] Parkinson disease (PD) is neurodegenerative disorder caused by the degeneration of dopaminergic neurons in nigrostriatal region of brain, and distinguished by malfunctioning of motor coordination apparent as tremor and rigidity of the limbs and trunk.[7] A$_{2A}$Rs have been recognized as potential therapeutic target for the treatment of PD.[8] Blockade of the A$_{2A}$Rs in striatopallidal neurons diminished postsynaptic effects of dopamine depletion, and in turn reduced the motor deficits of PD.[9] Besides providing symptomatic relief in PD, A$_{2A}$R antagonists have also been implemented to afford neuroprotection in various animal models of PD.[10,11]

Numerous potent and selective A$_{2A}$R antagonists (Fig. 1) of structural variability have been synthesized.[12–16] However, xanthine compounds such as KW6002 were unsuccessful in clinical trials[17] and non-xanthine compounds such as SCH58261 suffered from lower selectivity, poor solubility and poor pharmacokinetic profile.[18] Recently, thiazole derivatives have revealed their therapeutic potential in various diseases.[19,20] Thiazolo [4,5-*g*] dihydroindazoles, thiazolo [5,4-*b*] pyrimidine-5 (4*H*)-ones and thiazole [5,4-*f*] quinazolin-9-ones have exhibited PI$_3$ kinase modulatory, HIV-integrase inhibitory and GSK-3 inhibitory activities, respectively. Thiazolopyrimidine exhibited adenosine A$_3$ receptor antagonist activity[21] and monocyclic thiazoles have been reported to possess potential A$_{2A}$R antagonist activity.[22]

In the present work, we have designed novel thiazolotriazolopyrimidine derivatives as A$_{2A}$R antagonists based on non-xanthine tricyclic pharmacophore structural necessities such as tricyclic ring structure and furan ring.[15] The pharmacophore model Hypo-A$_{2A}$ established that minimal structural requirement features for A$_{2A}$R antagonistic activity and selectivity were aromatic ring (R), positively ionizable group (P), hydrophobicity (H), and hydrogen bond acceptor (L).[23] We replaced the pyrazole ring of SCH58261, a selective A$_{2A}$R antagonist by thiazole ring, and two categories of N-substituted thiazolotriazolopyrimidine derivatives were

* Corresponding author. Tel.: +91 11 27666272x231; fax: +91 11 27666248.
E-mail addresses: pmluthra@acbr.du.ac.in, pmlsci@yahoo.com (P.M. Luthra).
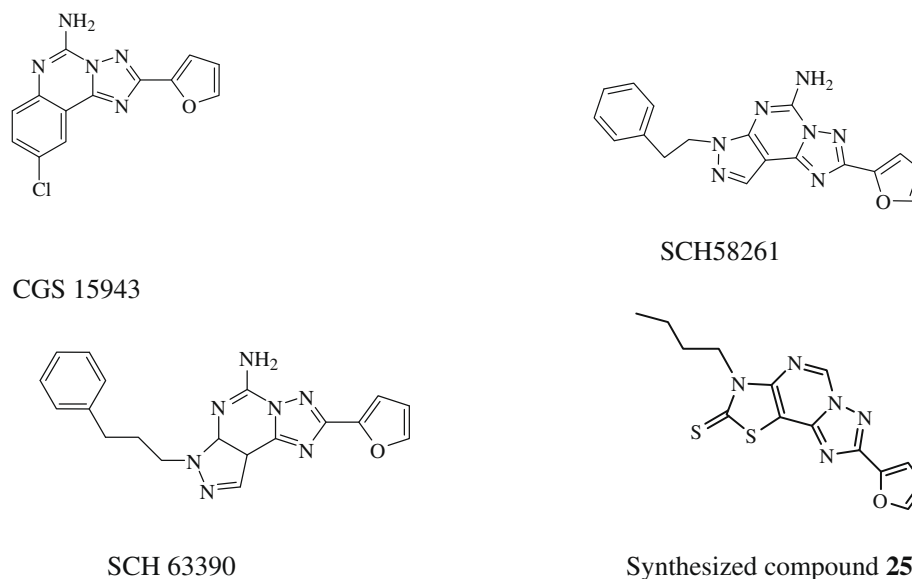
Figure 1. Structure of selective $A_{2A}R$ antagonist and synthesized compound.

prepared, one with flexible up to 4-carbon homologation, and other substituted and unsubstituted planar aromatic ring to give compounds (**23–33**). In silico interaction of the compounds (**23–33**) with $A_{2A}R$ was carried using autodock analysis. In vitro affinity and selectivity was determined by radioligand-binding assay in membranes isolated from stably transfected HEK293 cells with human $A_{2A}R$. Decrease in endogenous cAMP concentrations in treated HEK293 cells and restoration of locomotor activity in haloperidol-induced mice model was measured for most selective compounds possessing strong binding affinity to appraise their potential as $A_{2A}R$ antagonists.

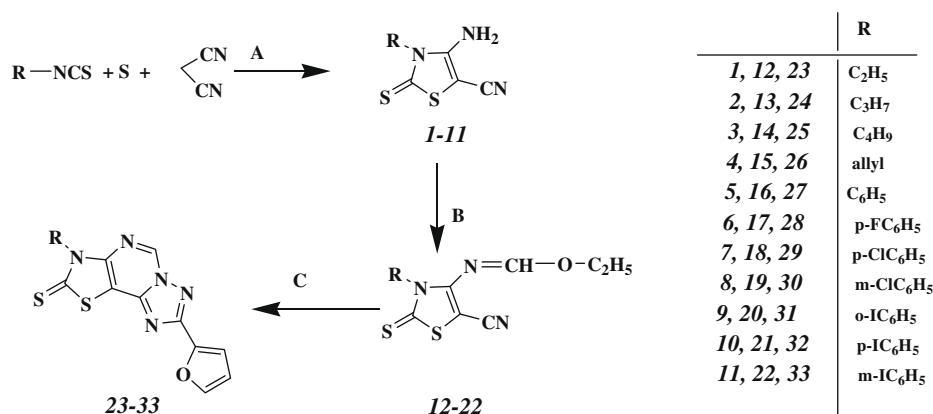## 2. Results and discussion

2.1. Synthesis

Synthesis of thiazolotriazolopyrimidine compounds (**23–33**) has been carried out according to Scheme 1. Concisely, the reaction of substituted isothiocyanate, triethylamine, sulfur and malononitrile was carried at 0–5 °C for 1 h, then at room temperature for an hour to give the carbonitrile compounds (**1–11**). The amino group of the carbonitrile substrates (**1–11**) was extended with triethyl orthoformate in toluene and p-toluenesulfonic acid (PTSA) to give

monocyclic thiazole compounds 4-ethoxymethylene-imino-3-substituted-2-thioxo-1,3-thiazole-5-carbonitriles (**12–22**), which were used as key intermediates in cyclization reactions. The formation of Schiff's bases (**12–22**) was confirmed on the basis of spectroscopic data. The disappearance of intense absorption band at 3230–3369 cm^{-1} for free amino group in IR spectra, and appearance of singlet for N=CH in ^{1}H spectra validated the formation of Schiff's bases (**12–22**). Condensation of monocyclic substrates **12–22** with 2-furoic acid hydrazide and isobutyric acid in toluene for 4 h gave tricyclic thiazolo[4,5-b] pyrimidine compounds (**23–33**) (Scheme 1). Disappearance of nitrile (–CN) absorption band at 2205 cm^{-1} in IR spectra and appearance of singlet for N=CH of pyrimidine ring in ^{1}H NMR spectra appeared to confirm the formation of cyclized tricyclic compounds (**23–33**).

2.2. Molecular docking study

To explicate the interaction of thiazolotriazolopyrimidine derivatives (**23–33**) with $A_{2A}R$, molecular docking analysis of the compounds **23–33** and known $A_{2A}R$ antagonist (SCH58261 and ZM241385) were carried out with recently solved X-ray crystal structure of human $A_{2A}R$ (PDB ID: 3EML). The $A_{2A}R$ (3EML) binding cavity composed of TM2 (A63, I66), TM3 (A81, V84, L85), ECL2

	R
1, 12, 23	C_2H_5
2, 13, 24	C_3H_7
3, 14, 25	C_4H_9
4, 15, 26	allyl
5, 16, 27	C_6H_5
6, 17, 28	p-FC_6H_5
7, 18, 29	p-ClC_6H_5
8, 19, 30	m-ClC_6H_5
9, 20, 31	o-IC_6H_5
10, 21, 32	p-IC_6H_5
11, 22, 33	m-IC_6H_5

Scheme 1. Reagent and condition: (A) triethyl amine; (B) tritethylorthoformate, p-toluenesulfonic acid (PTSA), reflux; (C) furoic acid hydrazide, isobutyric acid, 50 °C.

C. B. Mishra et al. / Bioorg. Med. Chem. 18 (2010) 2491–2500

2493

(F168, E169), ECL3 (H 264, W268), TM5 (M174, M177) and TM6 (W246, L249, N253) domains. Docking simulation results showed that thiazolotriazolopyrimidine derivatives (23–33) and SCH58261 shared a similar binding motif inside the transmembrane (TM) region and extracellular loops of the human $A_{2A}R$ similar to the co-crystallized ZM241385.[24] The binding interaction of thiazolo-triazolopyrimidine derivative 25 as one of the representatives showed that the ring sulfur and exocyclic sulfur of thiazolo ring were oriented towards the N253, M177 and V178 (Fig. 2). The involvement of thiazolo sulfurs in H-bond interaction with amide moiety of N253 was analogous to N-1 nitrogen at 7-position of ZM241385 and SCH58261 with $A_{2A}R$. Residue N181 was involved in H-bond formation with nitrogen of triazolo ring of thiazolotriazolopyrimidine, SCH58261 and ZM241385. Further key receptor residues F168, E169 from ECL2 form aromatic stacking and hydrophobic polar interaction with N1 position substituent of thiazolotriazolopyrimidine. The receptor residues F183, H250 were involved in the formation of H-bond with furan ring of thiazolotriazolopyrimidine, and the hydrophobic interaction of residues V84, L85, V86, L249, F182 in the vicinity of furan ring provided stability to hold the molecule in the cavity.[24,25] F168 (ECL2) provided aromatic stacking interaction with the tricyclic core, H250, W246 and N253 were associated with stabilizing the furan ring with mild polar interaction[24,25] (Fig. 3). Thiazolotriazolopyrimidine derivatives (23–33) possessed scaffolds orientation and contacts almost similar to SCH58261 and ZM241385. Moreover, the hydrophobic side chains of thiazolotriaz-olopyrimidine derivative were the deciding factor for their sitting conformation and affinity within the active site of $A_{2A}R$. Thiazolo ring N-substituent side chain ethyl, propyl, butyl, allyl and fluoro-benzene showed higher binding affinity that could be related to hydrophobicity and size of the substituent.

2.3. Structure–activity relationship

The results of $A_{2A}R$ binding assay are expressed as inhibition constants (K_i in nM). In the set of N-1 flexible side chains of thiaz-olotriazolopyrimidine derivatives, ethyl substitution (23) exhibited significantly higher binding affinity with A_1 receptor (0.096 nM) as compared to $A_{2A}R$ (3.56 nM). One carbon homologation gave pro-
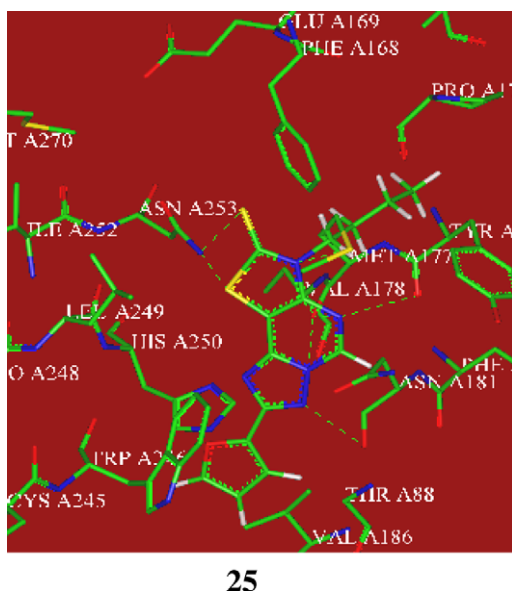

25

Figure 2. Hydrogen bond (H-bond) interactions (green dotted line) between compound 25 $A_{2A}R$ binding site residues. Residues and compounds are shown in stick representation. Nitrogen atoms are colored blue; oxygen atoms, red; and sulfur atoms, yellow.
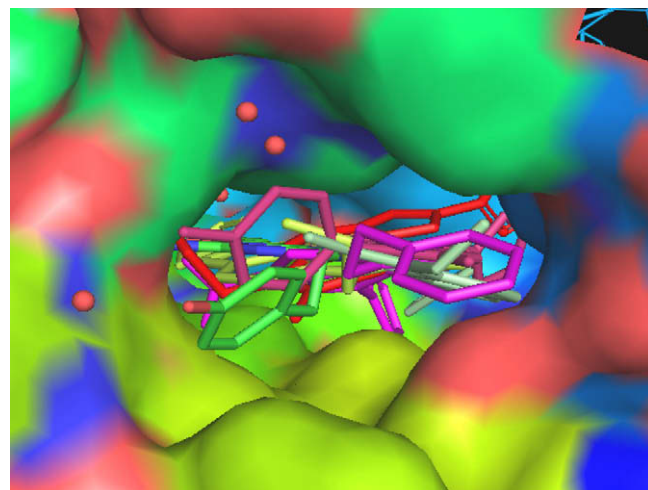

Figure 3. Molecular surface views of the active site of $A_{2A}R$ crystal structure, compounds are represented as stick. Butyl (red), fluoro (deep salmon), propyl (limon), SCH58261 (magenta), and ZM241385 (color by element i.e., CPK color) are docked in the binding pocket. The molecular surface is color-coded by hydropho-bicity properties. Basic amino acids (blue), acidic (red) and hydrophobic regions (yellow) aliphatic (green) water molecule (red dot).

pyl derivative of thiazolotriazolopyrimidine (24) with greatly improved binding affinity and selectivity with $A_{2A}R$ (634-fold selectivity over A_1 receptor). Further extending the alkyl chain to give butyl derivative of thiazolotriazolopyrimidine (25) showed reasonably good affinity (0.12 nM) and tremendous selectivity (1286-fold) compared to A_1 receptor. However 3-carbon chain with π-overlap in allyl derivative (26) led to excellent binding affinity (0.016 nM) and selectivity (1250-fold over A_1 receptor). In other set of compounds, incorporation of N-1 aromatic ring (phenyl) substituent (27) and p-fluorophenyl substitution (28) reduced binding affinity and selectivity. Chloro phenyl (m-, p-) and iodo phenyl (o-, p-) substitution showed significant affinity with $A_{2A}R$ and less selectivity over A_1, though m-iodo phenyl (33) substitution displayed both high binding affinity and selectivity (319.5-fold) towards $A_{2A}R$. The results from in silico and in vitro study accomplished that higher binding affinity of N-substituted thiazolo ring with propyl, butyl, allyl and p-fluorobenzene with $A_{2A}R$ could be due to their optimum topography at the binding site as compared to ethyl (23), phenyl (27), m- and p-chlorophenyl (29, 30), and o-, m- and p-iodophenyl (31–33) side chains. High selec-tivity of compounds 24–26 for $A_{2A}R$ could be related to specific lipophlilic interaction in the active site. m-Substituted phenyl derivative showed better affinity and selectivity for $A_{2A}R$ as compared to phenyl and p-substituted phenyl derivatives. Overall, alkyl derivatives (except ethyl) were more selective for $A_{2A}R$ than their aromatic counterparts (27–33) probably due to topographical parameter at the active site. Strong A_1R affinity of ethyl-substi-tuted thiazolotriazolopyrimidine indicates the conclusive role of C-length for receptor binding (see Table 1).

In functional assay, binding of ligands to $A_{2A}Rs$ promotes GPCR mediated conformational change via $G\alpha_s$ or $G\alpha_{i/o}$ subfamily to modulate the activity of adenylate cyclase and alter the concentra-tion of cAMP. An antagonist generally interacts with $A_{2A}R$ via $G\alpha_{i/o}$ subfamily to inhibit the activity of adenylate cyclase leading to de-crease in the cAMP concentration.[26] In our study, most selective compounds (24–26) treated with HEK293 cells stably transfected with human $A_{2A}R$ reduced the endogenous cAMP concentrations (0.10, 0.11 and 0.081 pmol/ml) further suggesting the $A_{2A}R$ antag-onist activity of the compounds. The degree of reduction in endog-enous cAMP concentration was significantly better than SCH58261

Table 1
Radioligand binding assay of thiazolotriazolopyrimidine compounds (**23–33**)
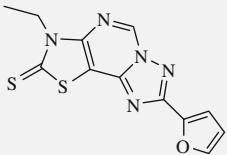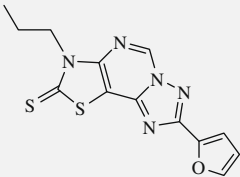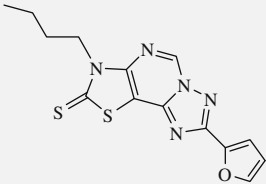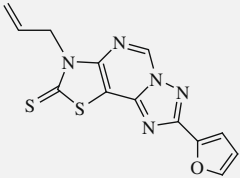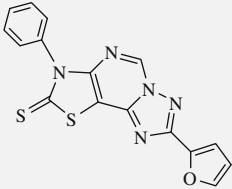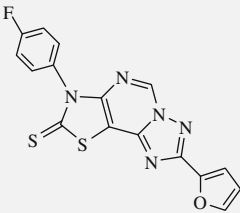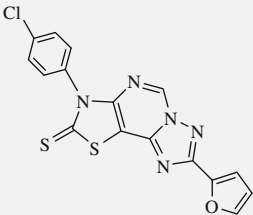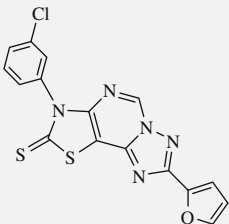
Compound	Structure	K_i (A$_{2A}$R) nM	K_i (A$_1$R) nM	A$_1$/A$_{2A}$
23		3.56	0.096	0.028
24		0.38	228.4	636.44
25		0.12	147.9	1286.09
26		0.016	19.01	1250.66
27		1.1	47.96	46.56
28		2.02	3.21	1.59
29		0.152	0.030	0.197
30		0.038	0.19	5

Table 1 (continued)

Compound	Structure	K_i (A_{2A}R) nM	K_i (A_1R) nM	A_1/A_{2A}
31		0.70	0.4	0.571
32		0.57	6.13	10.75
33		0.0082	2.62	319.5
SCH 58261		1.23	594.1	483

(0.25 pmol/ml), and higher than A_{2A}R agonist NECA (0.75 pmol/ml) and untreated cells (0.40 pmol/ml) (Table 2).

2.4. Haloperidol-induced catalepsy and akinesia

Haloperidol, a dopamine D_2 receptor antagonist blocks dopaminergic neurotransmission, induces catalepsy and akinesia causing the extrapyrimidal symptoms of PD and is employed to study PD in animal models. Catalepsy is condition characterized by muscular rigidity of posture regardless of external stimuli and akinesia is the inability to initiate movement. Blockade of A_{2A}Rs produces motor stimulant effects and reverses catalepsy induced by dopamine receptor blockade or by dopamine depletion.[27] Previously, it has been reported that A_{2A}R antagonists improve motor impairment in haloperidol-induced mice.[28] The effect of A_{2A}R antagonists on haloperidol-induced catalepsy has also been evaluated on primates.[29] In the present study, in vivo efficacy of the compounds **24–26** were assessed at various doses (5, 10 and 20 mg/kg (Supplementary data) by monitoring the restoration of locomotor activity (catalepsy and akinesia) in haloperidol-induced mice for 120 min. Thiazolotriazolopyrimidine derivatives (**24–26**) pre-treated haloperidol-induced (2.5 mg/kg) mice exhibited attenuation of catalepsy and akinesia (at doses 5, 10 and 20 mg/kg). The most effective dose for the compounds **24–26** was 10 mg/kg at which catalepsy score was comparable to SCH58261 (10 mg/kg (Table 3). The compound **24**

Table 2
cAMP functional assay of selected compounds (**24–26**)

Compounds	cAMP (pmol/ml)
Untreated cells	0.40
SCH58261	0.25
NECA	0.75
24	0.10
25	0.11
26	0.081

Table 3
Effect of selected compounds (**24–26**) on haloperidol-induced catalepsy

Compound	Dose (mg/kg bwt)	Time (min)						
		0	15	30	45	60	90	120
Saline			0	0	0	0	0	0
1% Acacia in saline			0	0	0	0	0	0
Haloperidol	2.5	0	0.625 ± 0.12	1.000 ± 0.20	1.375 ± 0.24	2.000 ± 0.29	2.625 ± 0.24	2.875 ± 0.12
SCH 58261	10	0	0	0	0.125 ± 0.12	0.250 ± 0.14	0.250 ± 0.14	0.625 ± 0.12
24	10	0	0	0.125 ± 0.12	0.250 ± 0.14	0.375 ± 0.12	0.500 ± 0.20	0.625 ± .12
25	10	0	0	0.125 ± 0.12	0.250 ± 0.14	0.375 ± 0.12	0.500 ± 0.20	0.750 ± 0.14
26	10	0	0	0.250 ± 0.14	0.250 ± 0.14	0.375 ± 0.12	0.625 ± 0.12	0.750 ± 0.14

Data represents the mean ± SEM; $n = 4$, $p \leqslant 0.05$ compared with control.

pre-treated mice (10 mg/kg) exhibited catalepsy score of 0.625 ± 0.12, which was similar to SCH58261 pre-treated mice. However, the compounds **25** and **26** pre-treated mice (10 mg/kg) displayed slightly higher catalepsy score (0.750 ± 0.14) than SCH58261 pre-treated mice. Vehicle groups saline and 1% acacia in saline exhibited catalepsy score of 0 and haloperidol treated group (2.5 mg/kg) represented catalepsy score of 2.875 ± 0.12. The three compounds showed comparative scores at different time intervals, however, the compound **24** showed lowest catalepsy score after 120 min. Significant attenuation in catalepsy score was observed in the compounds **24**, **25** and **26** as compared to haloperidol treated mice (Table 3).

The compound **24** pre-treated (10 mg/kg) haloperidol-induced mice showed akinesia score (39.50 ± 5.4 s) comparable to SCH58261 (10 mg/kg) pre-treated mice (32.25 ± 1.4 s). Whereas, compounds **25** and **26** (10 mg/kg) represented akinesia scores of 45.00 ± 3.8 s and 49.25 ± 5.8 s, respectively. The study demonstrated that the latency period was maximum in **26**, followed by **25** and **24**, however, was significantly lower in these three compounds as compared to haloperidol treated mice. Haloperidol treated mice (2.5 mg/kg) showed akinesia score of 119 ± 1 s and control groups saline and 1% acacia in saline exhibited 0 akinesia score after 120 min. Evidently, our results demonstrated that compound **24–26** antagonized the haloperidol-induced motor impairments (catalepsy and akinesia) (Tables 3 and 4).

3. Conclusion

We have reported the synthesis of new thiazolotriazolopyrimidine derivatives (**23–33**) and demonstrated their potential as potent and selective $A_{2A}R$ antagonists. In silico molecular docking study showed that strong interaction of the compounds (**23–33**) with $A_{2A}R$ were similar to standard antagonist SCH58261 as both shared identical active site binding pocket. All the compounds displayed significantly high binding affinity with $A_{2A}R$ in in vitro radioligand binding assay except three (**23, 29** and **31**). However, compounds **24–26** displayed both higher binding affinity and selectivity for $A_{2A}R$ in comparison to standard $A_{2A}R$ antagonist SCH58261 and antagonized the $A_{2A}R$-coupled release of endogenous cAMP from HEK293 cells. Our results demonstrated that blockade of $A_{2A}Rs$ by thiazolotriazolopyrimidines (**24–26**) antagonize haloperidol-induced hypo-locomotor behavior (catalepsy and akinesia) in vivo and produce motor stimulant effects to further accentuate their potential for treatment of PD symptoms.

4. Experimental

4.1. General

TLC was carried out on commercially available TLC silica gel (Silica Gel 60 F254) plates (Merck, Germany). The compounds were fully characterized by TLC, IR, ^{1}H NMR, ^{13}C NMR, and Mass spectroscopy. IR spectra were performed on Spectrum BX FTIR, Perkin Elmer. NMR spectra were recorded on AC Bruker 300 MHz spectrometer in CDCl$_3$ or DMSO. Mass spectra were recorded on a QSTAR XL LC–MS–MS, Applied Biosystem. Melting points were determined using model KSPII, KRUSS, Germany. Elemental analysis was performed on elementar analysensysteme. Column chromatography purifications were performed using silica gel Merck 100–200 mesh. Purity of the final step compounds was checked by HPLC (Shimadzu model 8A) using acetonitrile (98%) + methanol (2%) as mobile phase.

4.2. Synthesis of 4-amino-3-substituted-2-thioxo-1,3-thiazole-5-carbonitrile (1–11)

Synthesis of compounds **1–11** have been carried according to Luthra et al.[29] Briefly, an equimolar mixture of isothiocyanate, malononitrile and sulfur powder in dimethylformamide was stirred in ice bath. After 15 min, triethylamine was added drop-wise to the mixture, and the reaction was continued to 4 h. The reaction mixture was poured in water and precipitate was dissolved in absolute ethanol to give pure crystalline 4-amino-3-substituted-2-thioxo-2,3-dihydro-thiazole-5-carbonitrile derivatives (**1–11**).

4.2.1. 4-Amino-3-ethyl-2-thioxo-1,3-thiazole-5-carbonitrile (1)
Yield: 74%. White solid; mp: 205 °C. IR (KBr) 3308.95, 3227.11 (NH$_2$), 2973 (alkyl), 2206.84 (CN), 1193.14 (C=S) cm^{-1}. ^{1}H NMR (CDCl$_3$): δ 1.27–1.32 (t, J = 7.2 Hz, 3H, –CH$_3$), 4.22–4.29 (q, J = 7.2 Hz, 2H, CH$_2$), 6.38 (s, 2H, NH$_2$). ^{13}C NMR (CDCl$_3$): 16.5, 45.6, 118.4, 158.7, 118.4, 158.7, 190.8. LC–MS: m/z 185 (M$^+$), 186 (M+1).

4.2.2. 4-Amino-3-propyl-2-thioxo-1,3-thiazole-5-carbonitrile (2)
Yield: 85%. White solid; mp: 160 °C. IR (KBr), 3319.65, 3234.59 (NH$_2$), 2205.95 (CN), 1198.14 (C=S) cm^{-1}. ^{1}H NMR (CDCl$_3$): δ 1.03 (t, J = 7.5, 3H, CH$_3$), 1.72–1.854 (m, 2H, CH$_2$), 4.10 (t, J = 7.8 Hz, 2H, CH$_2$), δ 4.83 (s, 2H, NH$_2$). ^{13}C NMR (CDCl$_3$): 11.2, 20.3, 47.9, 118, 151.9, 186. LC–MS: m/z 199 (M$^+$), 200 (M+1).

4.2.3. 4-Amino-3-butyl-2-thioxo-1,3-thiazole-5-carbonitrile (3)
Yield: 84%. Brown solid; mp: 155 °C. 3320.05, 3234.19 (NH$_2$), 2208.95 (CN), 1199.14 (C=S) cm^{-1}. ^{1}H NMR (300 MHz, CDCl$_3$) δ 0.97 (t, J = 7.2 3H, CH$_3$), 1.353–1.476 (m, 2H, CH$_2$), 1.66–1.74 (m, 2H, CH$_2$), 4.16 (t, J = 7.8 Hz, 2H, CH$_2$), 6.120 (s, 2H, NH$_2$). LC–MS: m/z 213 (M$^+$), 214 (M+1).

4.2.4. 4-Amino-3-allyl-2-thioxo-1,3-thiazole-5-carbonitrile (4)
Yield: 72%. Yellow solid; mp: 170–172 °C IR (KBr), 3313.65, 3224.89 (NH$_2$), 2194.95 (CN), 1193.14 (C=S) cm^{-1}. ^{1}H NMR (CDCl$_3$): δ 4.88 (d, J = 4.8 Hz, 2H, CH$_2$), 5.35 (d, J = 1.5 Hz, 2H, CH$_2$), 5.77–5.89 (m, 1H, CH), 6.50 (s, 2H, NH$_2$). LC–MS: m/z 197 (M$^+$), 198 (M+1).

Table 4
Effect of selected compounds (**24–26**) on haloperidol-induced akinesia

Compound	Dose (mg/kg bwt)	Time (min)						
		0	15	30	45	60	90	120
Saline		0	0	0	0	0	0	0
1% Acacia in saline		0	0	0	0	0	0	0
Haloperidol	2.5	0	78 ± 12.6	111 ± 5.4	112 ± 5.2	118 ± 2	119 ± 1	119 ± 1
SCH 58261	10	0	0	0.75 ± 0.75	6.50 ± 2.3	16.50 ± 4.4	26.25 ± 3.4	32.25 ± 1.4
24	10	0	0	6.00 ± 3.5	7.75 ± 3.3	16.50 ± 3.8	26.25 ± 4.9	39.50 ± 5.4
25	10	0	0	4.75 ± 2.7	15.00 ± 3.6	24.25 ± 4.4	33.50 ± 2.9	45.00 ± 3.8
26	10	0	0	6.00 ± 3.5	21.25 ± 4.3	33.00 ± 2.8	41.50 ± 3.1	49.25 ± .8

Data represents the mean ± SEM; n = 4, p ⩽ 0.05 compared with control.

4.2.5. 4-Amino-3-phenyl-2-thioxo-1,3-thiazole-5-carbonitrile (5)

Yield: 75%. Yellow solid; mp: 286 °C. IR (KBr): 3369, 3230 (NH$_2$), 2204 (CN), 684 (C–S–C) cm^{-1}. ^{1}H NMR (300 MHz, CDCl$_3$): δ 5.90 (s, 2H, NH$_2$) 7.12–7.47 (m, 5H, Ar). ^{13}C NMR (75 MHz, CDCl$_3$): δ 112.2, 130.8, 131.1, 132.9, 133.7, 154.3, 188.1. LC–MS: m/z 233 (M$^+$).

4.2.6. 4-Amino-3-(p-fluorophenyl)-2-thioxo-1,3-thiazole-5-carbonitrile (6)

Yield: 65%. Yellow solid; mp: 219 °C. IR (KBr) 3352.61, 3248.85 (NH$_2$), 2206.30 (CN), 1272.04 (C=S) cm^{-1}. ^{1}H NMR (300 MHz, CDCl$_3$): δ 5.968 (s, 2H, NH$_2$), 7.29–7.37 (m, 4H, Ar). LC–MS: m/z 251 (M$^+$), 252 (M+1).

4.2.7. 4-Amino-3-(p-chlorophenyl)-2-thioxo-1,3-thiazole-5-carbonitrile (7)

Yield: 55%. Yellow solid; mp: 172–173 °C. IR (KBr) 3298.61, 3234.85 (NH$_2$), 2204.30 (CN), 1244.04 (C=S), 744 (C–Cl) cm^{-1}. ^{1}H NMR (300 MHz, CDCl$_3$) δ 6.61 (s, 1H, NH$_2$) 7.27 (d, J = 8.1 Hz, 2H, Ar), 7.33 (d, J = 7.8 Hz. 2H, Ar). LC–MS: m/z 267 (M$^+$), 268 (M+1).

4.2.8. 4-Amino-3-(m-chlorophenyl)-2-thioxo-1,3-thiazole-5-carbonitrile (8)

Yield: 56%. Brown solid; mp: 178–180 °C. IR (KBr) 3299.81, 3236.85 (NH$_2$), 2206 (CN), 1248.04 (C=S), 748 (C–Cl) cm^{-1}. ^{1}H NMR (300 MHz, CDCl$_3$): δ 5.92 (s, 2H, NH$_2$), 7.26–7.51 (m, 4H). LC–MS: m/z 267 (M$^+$), 268 (M+1).

4.2.9. 4-Amino-3-(o-iodophenyl)-2-thioxo-1,3-thiazole-5-carbonitrile (9)

Yield: 48%. Yellow solid; mp: 238 °C. IR (KBr) 3329.61, 3234.85 (NH$_2$), 2201.30 (CN), 1276.04 (C=S) cm^{-1}. ^{1}H NMR (300 MHz, CDCl$_3$): δ 4.58 (s, 2H, NH$_2$), 7.37–7.70 (m, 4H, Ar). LC–MS: m/z 360 (M+1).

4.2.10. 4-Amino-3-(p-iodophenyl)-2-thioxo-1,3-thiazole-5-carbonitrile (10)

Yield: 45%. Red solid; mp: 228–230 °C. IR (KBr) 3328.61, 3236.85 (NH$_2$), 2201.30 (CN), 1278.04 (C=S) cm^{-1}. ^{1}H NMR (300 MHz, CDCl$_3$): δ 5.96 (s, 1H, NH$_2$), 7.35 (d, 2H, Ar), 7.57 (d, 2H, Ar). LC–MS m/z 360 (M+1).

4.2.11. 4-Amino-3-(m-iodophenyl)-2-thioxo-1,3-thiazole-5-carbonitrile (11)

Yield: 45%. Red solid; mp: 230–232 °C. IR (KBr) 3328.62, 3236.85 (NH$_2$), 2201.30 (CN), 1278.04 (C=S) cm^{-1}. ^{1}H NMR (300 MHz, DMSO): δ 7.61–7.26 (m, 3H, Ar), 7.95 (d, 1H, J = 8.7Hz, Ar). LC–MS m/z 360 (M+1).

4.3. 4-(Ethoxymethylene) amino-3-substituted-2-thioxo-1, 3-thiazole-5-carbonitrile (12–22)

Compounds **12–22** have been synthesized according to Luthra et al.[30] Concisely, the carbonitrile compounds (**1–11**) were refluxed with triethylorthoformate (equal equivalents) and PTSA (catalytic amount) in toluene for 6 h. The reaction mixture was poured in water, toluene layer was separated and washed with water, dried with Na$_2$SO$_4$. The crude product was purified by column chromatography to give viscous liquid compounds (**11, 13, 14** and **17–22**) and solid products (**12, 15** and **16**). Solid compounds were re-crystallized from absolute ethanol.

4.3.1. 4-(Ethoxymethylene)-amino-3-(ethyl)-2-thioxo-1,3-thiazole-5-carbonitrile (12)

Yield: 75%. Yellow crystal; mp: 116 °C. IR (KBr) 2962.13, 2852 (alkyl), 2209.28 (CN), 1228 (C=S) cm^{-1}. ^{1}H NMR (CDCl$_3$): δ 1.27 (t, J = 7.2 Hz, 3H, CH$_3$), 1.46 (t, J = 7.2 Hz, 3H, CH$_3$), 4.44 (q, J = 7.2 Hz, 2H, CH$_2$), 4.47 (q, J = 7.2 Hz, 2H, CH$_2$), 8.332 (N=CH). ^{13}C NMR (CDCl$_3$): 12.4, 13.8, 41.6, 42.5, 65.2, 112.0, 161.5, 185.9. LC–MS: m/z 242 (M+1).

4.3.2. 4-(Ethoxymethylene)-amino-3-(-propyl)-2-thioxo-1,3-thiazole-5-carbonitrile (13)

Yield: 86%. Yellow viscous liquid; IR (KBr) 2952.36, 2854.68 (alkyl), 2208.00 (CN), 1265.12 (C=S) cm^{-1}. ^{1}H NMR (CDCl$_3$): δ 0.87 (t, J = 7.2 Hz, 3H, CH$_3$), 1.16 (t, J = 7.2 Hz, 3H, CH$_3$), 2.27–2.38 (m, 2H, CH$_2$), 3.99 (q, J = 7.2 Hz, 2H, CH$_2$), 4.22 (t, J = 7.5 Hz, 2H, CH$_2$), 7.96 (s, 1H, N=CH). LC–MS: m/z 256 (M+1).

4.3.3. 4-(Ethoxymethylene)-amino-3-(butyl)-2-thioxo-1,3-thiazole-5-carbonitrile (14)

Yield: 85%. Yellow viscous liquid; IR (KBr) 2956.36, 2865.32 (Alkyl), 2212.26 (CN), 1268.66 (C=S) cm^{-1}. ^{1}H NMR (CDCl$_3$): δ 0.98 (t, J = 6.6 Hz, 3H, CH$_3$), 1.27–1.29 (m, 2H, CH$_2$), 1.29 (t, J = 7.2 Hz, 3H, CH$_3$), 1.51–1.53 (m, 2H, CH$_2$), 4.09 (q, J = 7.2 Hz, 2H, CH$_2$), 4.46 (t, J = 6.9 Hz, 2H, CH$_2$), 8.13 (s, 1H, N=CH). LC–MS: m/z 270 (M+1).

4.3.4. 4-(Ethoxymethylene)-amino-3-(allyl)-2-thioxo-1,3-thiazole-5-carbonitrile (15)

Yield: 65%. Yellow crystals; mp: 122–124 °C. 2958.06, 2851.08 (alkyl), 2206.56 (CN), 1268 (C=S) cm^{-1}. ^{1}H NMR (CDCl$_3$): δ 1.44 (t, J = 7.2 Hz, 3H, CH$_3$), 4.46 (q, J = 7.2 Hz, 2H, CH$_2$), 4.79 (d, J = 4.5 Hz, 2H, CH$_2$), 5.25 (d, J = 0.9 Hz, 2H, CH$_2$), 5.76–5.89 (m, 1H, CH), 8.26 (s, 1H, N=CH). LC–MS: m/z 254 (M+1).

4.3.5. 4-(Ethoxymethylene)-amino-3-(phenyl)-2-thioxo-1,3-thiazole-5-carbonitrile (16)

Yield: 55%. Yellow crystal; mp: 116 °C. IR (KBr) 2208.00 (CN), 1250.18 (C=S) cm^{-1}. ^{1}H NMR (CDCl$_3$) δ: 1.12 (t, J = 7.2 Hz, 3H, CH$_3$), 4.04 (q, J = 7.2 Hz, 2H, CH$_2$), 7.17–7.26 (m, 2H, Ar), 7.46–7.56 (m, 3H, Ar), 8.16 (s, 1H, N=CH). LC–MS: m/z 289 (M$^+$), 290 (M+1).

4.3.6. 4.3.64-(Ethoxymethylene)-amino-3-(p-fluorophenyl)-2-thioxo-1,3-thiazole-5-carbonitrile (17)

Yield: 55%. Yellow viscous liquid; IR (KBr) 2950.12, 2842.88 (alkyl), 2204.08 (CN), 1262.00 (C=S) cm^{-1}. ^{1}H NMR (CDCl$_3$): δ 1.27 (t, J = 7.2 Hz, 3H, CH$_3$), 4.18 (q, J = 7.2 Hz, 2H, CH$_2$), 7.43 (d, J = 8.1, 2H, Ar), 7.75 (d, 2H, J = 8.1, 2H, Ar), 8.03 (s, 1H, N=CH). ^{13}C NMR (CDCl$_3$). LC–MS: m/z 308 (M+1).

4.3.7. 4-(Ethoxymethylene)-amino-3-(p-chlorophenyl)-2-thioxo-1,3-thiazole-5-carbonitrile (18)

Yield: 52%, Yellow viscous liquid. IR (KBr), 2956.23, 2862.12 (alkyl), 2202 (CN), 1262 (C=S) cm^{-1}. ^{1}H NMR (CDCl$_3$): δ 1.29 (t, J = 7.2 Hz, 3H, CH$_3$), 4.19 (q, J = 7.2 Hz, 2H, CH$_2$), 7.31–7.52 (m, 4H, Ar), 8.04 (s, 1H, N=CH). LC–MS m/z 323 (M$^+$), 324 (M+1).

4.3.8. 4-(Ethoxymethylene)-amino-3-(m-chlorophenyl)-2-thioxo-1,3-thiazole-5-carbonitrile (19)

Yield: 52%. Yellow viscous liquid, IR (KBr) 2942.23, 2844.43, (alkyl) 2202 (CN), 1265 (C=S). ^{1}H NMR (CDCl$_3$): δ 1.16 (t, J = 6.9 Hz, 3H, CH$_3$), 4.41 (q, J = 6.9 Hz, 2H, CH$_2$), 7.47–7.53 (m, 3H, Ar), 7.80 (d, J = 8.1, 1H, Ar), 8.44 (s, 1H, N=CH). LC–MS: m/z 324 (M+1).

4.3.9. 4-(Ethoxymethylene)-amino-3-(o-iodophenyl)-2-thioxo-1,3-thiazole-5-carbonitrile (20)

Yield: 54%. Yellow viscous liquid IR (KBr), 2952, 2802 (alkyl), 2205 (CN), 1257 (C=S) cm^{-1}. ^{1}H NMR (CDCl$_3$): δ 1.28 (t, J = 7.2 Hz, 3H, CH$_3$), 4.20 (q, J = 7.2 Hz, 2H, CH$_2$), 7.38–7.62 (m, 4H, Ar), 8.03 (s, 1H, N=CH). LC–MS (EI, 70 eV). m/z 415 (M+1).

4.3.10. 4-(Ethoxymethylene)-amino-3-(p-iodophenyl)-2-thioxo-1,3-thiazole-5-carbonitrile (21)

Yield: 54%. Yellow viscous liquid IR (KBr), 2952, 2802 (alkyl), 2205 (CN), 1257 (C=S) cm^{-1}. ^{1}H NMR (CDCl$_3$): δ 1.29 (t, J = 7.2 Hz, 3H, CH$_3$), 4.28 (q, J = 7.2 Hz, 2H, CH$_2$), 7.35 (d, J = 8.4 Hz, 2H, Ar), 7.60 (d, J = 8.4 Hz, 2H, Ar), 8.12 (s, 1H, N=CH). LC–MS: m/z 415 (M+1).

4.3.11. 4.3.11.4-(Ethoxymethylene)-amino-3-(m-iodophenyl)-2-thioxo-1,3-thiazole-5-carbonitrile (22)

Yield: 65%. Yellow viscous liquid IR (KBr) 2962.20, 2857 (alkyl), 2206 (CN), 1272 (C=S) cm^{-1}. ^{1}H NMR (CDCl$_3$): δ 1.06 (t, J = 6.9 Hz, 3H, CH$_3$), 4.07 (q, J = 6.9 Hz, 2H, CH$_2$), 7.49–7.51 (m, 3H, Ar), 7.79 (d, J = 8.1, 1H, Ar), 8.4 7 (s, 1H, N=CH) LC–MS: m/z 415 (M+1).

4.4. Synthesis of 8-(2-thioxo-7-(3-substituted-2-(2-furyl) thiazolo [4,e]-1,2,4-triazolo [1,5-c] pyrimidine (23–33)

Synthesis of compounds **23–33** have been carried according to Shaker et al.[31] with minor modifications. An equivalent mixture of imino-ether derivatives (**12–22**) in toluene, 2-furoic acid hydrazide and isobutyric acid was stirred at 60 °C for 1–2 h. The reaction continued with azeotropic removal of water. The precipitate was filtered and washed with absolute hot ethanol and dried. The crude product was purified by column chromatography and re-crystallized to give pure tricyclic compound (**23–33**).

4.4.1. 8-(2-Thioxo-7(3-ethyl)-2-(2-furyl) thiazolo [4,3-e] 1,2,4-triazolo[1,5-c] pyrimidine (23)

Yield: 72%. White solid; mp: 248 °C IR (KBr) 2981.66, 2788.39 (alkyl), 1253 (C=S), 3064.43 (Ar, CH) cm^{-1}. ^{1}H NMR (300 MHz, CDCl$_3$): δ 1.44 (t, J = 7.2 Hz, 3H, CH$_3$). 4.62 (q, J = 7.2 Hz, 2H, CH$_2$), 6.63 (q, J = 1.5 Hz, 1H, Ar), 7.31 (d, J = 3 Hz, 1H, Ar), 7.68 (s, 1H,Ar), 9.26 (s, 1H, N=CH). ^{13}C NMR (CDCl$_3$): 12.3, 41.9, 112.2, 113.9, 138.7, 144.7, 145.7, 147.1, 149.2, 159.1, 187.1. LC–MS: m/z 303 (M$^+$), 304 (M+1). HPLC purity 100%.

4.4.2. 8-(2-Thioxo-7(3-propyl)-2-(2-furyl) thiazolo [4,3-e] 1,2,4-triazolo[1,5-c] pyrimidine (24)

Yield: 76%. White solid mp: 245 °C IR (KBr) 2965.13, 2330.96, 2870.84 (alkyl), 1226 (C=S), 3071 (Ar, CH) cm^{-1}. ^{1}H NMR (300 MHz, CDCl$_3$): δ 1.04 (t, J = 7.5 Hz, 3H, CH$_3$), 1.84–1.97 (m, 2H, CH$_2$), 4.50 (q, J = 7.5 Hz, 2H, CH$_2$), 6.62 (q, J = 1.8 Hz, 1H, Ar), 7.30 (d, J = 2.7 Hz, 1H, Ar), 7.67 (d, J = 0.6 Hz, 1H, Ar), 9.22 (s, 1H, N=CH). ^{13}C NMR (CDCl$_3$): 11.2, 20.5, 48.2, 106.4, 112.2, 113.3, 138.5, 144.7, 145.4, 147.3, 149.4, 159.5, 187.9.LC–MS: m/z 317 (M$^+$), 318 (M+1). HPLC purity 100% Anal. Calcd for C$_{13}$H$_{11}$N$_5$OS$_2$: C, 49.19; H, 3.49; N, 22.07; S, 20.21. Found: C, 48.97; H, 3.41; N, 21.87; S, 20.05.

4.4.3. 8-(2-Thioxo-7(3-butyl)-2-(2-furyl),thiazolo,[4,3-e]1,2,4-triazolo[1,5-c] pyrimidine (25)

Yield: 84%. White solid; mp: 220 °C IR (KBr), 2961, 2927, 2856 (Butyl). 1190 (C=S) cm^{-1}. ^{1}H NMR (300 MHz, CDCl$_3$): δ 1.00 (t, J = 7.5, 3H, CH$_3$), 1.40–1.53 (m, 2H, CH$_2$), 1.79–1.89 (m, 2H, CH$_2$), 4.50 (t, J = 7.5 Hz, 2H, CH$_2$), 6.63 (q, J = 1.8 Hz, 1H, Ar), 7.29 (d, J = 3.3 Hz, 1H, Ar), 7.67 (d, J = 0.6 Hz, 1H, Ar), 9.28 (s, 1H, N=CH). ^{13}C NMR (CDCl$_3$): 13.7, 20.0, 29.6, 46.6, 106.4, 112.2, 113.9, 138.5, 144.7, 145.4, 147.3, 149.4, 159.5, 187.8. LC–MS (m+1) LC–MS: m/z 331 (M$^+$), 332 (M+1). HPLC purity 100% Anal. Calcd for C$_{14}$H$_{13}$N$_5$OS$_2$: C, 50.74; H, 3.95; N, 21.13; S, 19.35. Found: C, 50.54; H, 3.82; N, 21.02; S, 19.29.

4.4.4. 8-(2-Thioxo-7(3-allyl)-2-(2-furyl) thiazolo [4,3-e] 1,2,4-triazolo [1, 5-c] pyrimidine (26)

Yield: 63%. White solid; mp: 253 °C IR (KBr), 1635 (C=C), 1262 (C=S), 3033.21 (Ar, CH) cm^{-1}. ^{1}H (300 MHz, CDCl$_3$): δ 5.16 (d,

J = 4.5 Hz, 1H, CH$_2$). 5.29 (d, J = 0.9 Hz, 2H, CH$_2$), 5.93–6.06 (m, 1H, CH), 6.66 (q, J = 1.5 Hz, 1H, Ar), 7.31 (d, J = 3.3 Hz, 1H, furan), 7.67 (s, 1H, Ar), 9.23 (1H, N=CH). ^{13}C NMR (CDCl$_3$): 48.3, 106.2, 112.2, 114.0, 119.9, 129.2, 138.7, 144.7, 145.4, 149.1, 159.5, 187.8. LC–MS: m/z 315 (M$^+$), 316 (M+1). HPLC purity 100% Anal. Calcd for C$_{13}$H$_9$N$_5$OS$_2$: C, 49.51; H, 2.88; N, 22.21; S, 20.33. Found: C, 49.48; H, 2.81; N, 21.94; S, 20.28.

4.4.5. 8-(2-Thioxo-7-(3-phenyl)-2-(2-furyl) thiazolo [4,3-e]1,2,4-triazolo[1,5-c] pyrimidine (27)

Yield: 62%. White solid; mp: 298–299 °C. IR (KBr), 3059 (Aromatic CH), 1222 (C=S) cm^{-1}. ^{1}H NMR (300 MHz, CDCl$_3$): δ 6.65 (d, J = 1.5 Hz, 1H,), 7.32 (d, J = 3.6 Hz, 1H furan), 7.42–7.68 (m, 6H, Ar, H), 9.13 (s, 1H, N=CH). LC–MS: m/z 351 (M$^+$), 352 (M+1). HPLC purity 100%.

4.4.6. 8-(2-Thioxo-7(3-p fluorophenyl)-2-(2-furyl) thiazolo [4,3-e] 1,2,4-triazolo[1,5-c] pyrimidine (28)

Yield: 75%. White solid; mp: 260 °C IR (KBr) 3036 (Ar, CH), 1260 (C=S) 1412 (C–F) cm^{-1}. ^{1}H NMR (300 MHz, CDCl$_3$): δ 6.63 (q, J = 1.8 Hz, 1H, Ar), 7.30–7.44 (m, 5H, Ar), 7.68 (t, J = 1.5 Hz, Ar) 9.13 (S, 1H, N=CH). ^{13}C NMR (CDCl$_3$): 106.4, 112.2, 114.0, 116.8, 117.1, 130.4, 130.5, 138.9, 144.5, 145.4, 147.4, 149.1, 159.6, 188.4. LC–MS: m/z 369 (M$^+$), 370 (M+1). HPLC purity 99.5%.

4.4.7. 8-(2-Thioxo-7(3-p-chlorophenyl.)-2-(2-furyl) thiazolo [4,3-e] 1, 2 4-triazolo [1,5-c] pyrimidine (29)

Yield: 54%. White solid; mp: 280 °C IR (KBr) 1119 (C–Cl), 3033.21 (Ar, CH), 1262 (C=S) cm^{-1}. ^{1}H NMR (300 MHz, CDCl$_3$): δ 6.57 (s, 1H, furan), 7.10 (d, J = 7.8 Hz, 2H, Ar), 7.36 (d, J = 3.3 Hz, 1H, Ar), 7.61 (s, 1H), 7.91 (d, J = 7.8 Hz, 2H, Ar), 9.05 (s, 1H, N=CH). ^{13}C NMR (CDCl$_3$): 106.9, 112.3, 114.1, 116.8, 117.2, 130.6, 131.8, 139.0, 144.8, 145.9, 147.3, 149.2 161.2, 190.2. LC–MS: m/z 385 (M$^+$), 386 (M+1). HPLC purity 100%.

4.4.8. 8-(2-Thioxo-7(3-m-chlorophenyl)-2-(2-furyl) thiazolo [4,3-e] 1,2,4-triazolo[1,5-c] pyrimidine (30)

Yield: 55%. White solid; mp 275 °C, IR (KBr) 1122 (C–Cl), 3035 (Ar, CH), 1265 (C=S) cm^{-1}. ^{1}H NMR (300 MHz, CDCl$_3$): δ 6.64 (q, J = 1.8 Hz, 1H, Ar), 7.44 (d, J = 3 Hz, 1H Ar), 7.51 (d, J = 0.9 Hz, 1H, Ar), 7.5 6–7.65 (m, 3H, Ar), 7.69 (s, 1H, Ar,) 9.20 (s, 1H, N=CH). ^{13}C NMR (CDCl$_3$): 106.8, 112.3, 114.1, 128.4, 130.6, 131.8, 138.9, 144.6, 145.3, 147.3, 159.3, 189.2. LC–MS: 385 (M$^+$), m/z 386 (M+1). HPLC purity 100%.

4.4.9. 8-(2-Thioxo-7(3-o-iodophenyl)-2-(2-furyl) thiazolo [4,3-e] 1,2,4-triazolo[1,5-c]pyrimidine (31)

Yield: 65%. White solid; mp: 316–317 °C IR (KBr), 3031 (Ar, CH), 1208 (C=S) cm^{-1}. ^{1}H NMR (300 MHz, DMSO): δ 6.75 (s, 1H, Ar), 7.36–7.65 (m, 5H, Ar), 7.98 (s, 1H, Ar), 9.68 (s, 1H, N=CH). LC–MS: m/z 477 (M$^+$), 478 (M+1). HPLC purity 97.1%.

4.4.10. 8-(2-Thioxo-7(3-p-iodophenyl)-2-(2-furyl) thiazolo [4,3-e] 1,2,4-triazolo[1,5-c] pyrimidine (32)

Yield: 63%. White solid; mp: 302 °C IR (KBr) 3036 (Ar, CH), 1094 (C–I), 1259 (C=S) cm^{-1}. ^{1}H NMR (300 MHz, CDCl$_3$): δ 6.63 (d, J = 1.5 Hz, 1H, Ar), 7.32 (d, J = 3 Hz, 1H, furan), 7.38 (d, J = 8.7 Hz, 2H, Ar), 7.62 (d, J = 8.4 Hz, 2H, Ar), 7.68 (s, 1H, furan), 9.13 (s, 1H, N=CH). ^{13}C NMR (CDCl$_3$): 106.6, 112.3, 114.1, 129.8, 130.3, 133.6, 136.4, 138.8, 144.6, 145.5, 147.29, 149.7, 159.8, 188.8. LC–MS: m/z 477 (M$^+$), 478 (M+1). HPLC purity 100%

4.4.11. 8-(2-Thioxo-7(3-m-iodophenyl)-2-(2-furyl) thiazolo [4,3-e] 1,2,4-triazolo[1,5-c]pyrimidine (33)

Yield: 63%. White solid; mp: 312–313 °C IR (KBr), 3031.30 (Ar, CH), 1208 (C=S) cm^{-1}. ^{1}H NMR (300 MHz, CDCl$_3$): δ 6.64 (d,

J = 1.5 Hz, 1H, Ar), 7.32–7.44 (m, 3H, Ar), 7.68 (s, 1H), 7.77 (s, 1H, Ar), 7.92 (d, 1H, Ar), 9.17 (s, 1H, Ar). ^{13}C NMR (CDCl$_3$): 106.6, 112.3, 114.1, 127.9, 131.2, 136.2, 137.3, 138.9, 139.3, 144.7, 145.5, 149.6, 159.7,188.8.LC–MS (EI-70 eV): m/z 477 (M$^+$), 478 (M+1). HPLC purity 99.7%.

4.5. Molecular docking

Docking simulations were performed with AutoDock3.0.5.[32] The recently solved X-ray crystal structure of the human A$_{2A}$R (pdb code: 3EML; 2.6-Å resolution) in complex with ZM241385 was retrieved from the RCSB Protein Data Bank and all heteroatoms were removed. The A$_{2A}$R was set up for docking with standard protocol. Polar hydrogens were added using PROTONATE utility distributed with AutoDock3.0.5 then protein coordinates were subjected to minimize with CHARMm force field potential.[33,34] Steps (1000) of steepest descent followed by conjugate gradient minimization until the RMS gradient of the potential energy was less than 0.05 kJ mol^{-1} Å^{-1} performed the minimizations. Kollman united atom charges and solvation parameters were added to the final protein file. The known A$_{2A}$R antagonists and thiazolotriazolopyrimidine derivatives were drawn on BUILDER module (Insight II). DISCOVER molecular dynamics (CHARMm force field) was run to carry the optimization of the ligands, which were saved in mol2 format with the aid of BABEL programs (Pat Walters and Matt Stahl, NCI). Full hydrogens were added to the ligands and Gasteiger-Marsili partial atomic charges were computed using the BABEL program and saved in the PDBQ format. All possible flexible torsions of the resultant ligand molecules were defined by using AUTOTORS. The prepared ligands in PDBQ format were used as input files for AutoDock3.0.5 in the next step. Docking simulation was carried out using the Lamarckian Genetic Algorithm.[32] For binding energy, three terms were taken into account in the docking step: the van der Waals interaction represented as a Lennard-Jones 12–6 dispersion/repulsion term, the hydrogen bonding represented as a directional 12–10 term, and the Coulombic electrostatic potential. The resulting docking orientations lying within 2.0 Å in the root-mean square deviation (rmsd) tolerance of each other were clustered together represented by the result with the most favorable free energy of binding. Finally, the obtained top-posed docking conformations were subjected to post-docking energy minimization on Insight-II/Accelrys.[33]

4.6. Radioligand binding assay

Adenosine A$_{2A}$R and A$_1$R binding assays: [^{3}H]ZM241385 and [^{3}H]DPCPX binding assays for adenosine A$_{2A}$R and A$_1$Rs, respectively, were performed in stably transfected HEK293 cells (procured from National Center for Cell Sciences, Pune, India) with human A$_{2A}$R and A$_1$R. Briefly, 10 μg HEK293 cell membranes isolated from were incubated with different concentrations (1 pM–1 μM) of compounds and 1 nM [^{3}H]ZM241385 in 200 μl incubation buffer containing 50 mM Tris-Cl, 1 mM EDTA, pH 7.4 and 2.5 U/ml adenosine deaminase. Adenosine A$_1$R assays were performed on 10 μg of HEK293 cell membranes expressing human adenosine A$_1$Rs and 1 nM [^{3}H]DPCPX in 200 μl incubation buffer. Reactions were carried out for 60 min at 26 °C and were terminated by rapid filtration over 96-well plates equipped with GF/B filters (Milipore, USA). Filters were washed three times with 300 μl of cold washing buffer containing 50 mM Tris-Cl, 10 mM MgCl$_2$, pH 7.4, air dried, and radioactivity retained on filters were counted in 1450 LSC& Luminescence counter (Wallac Microbeta Trilux, Perkin–Elmer, USA). The K_d values for radioligands [^{3}H]ZM241385 and [^{3}H]DPCPX were 0.99 and 1.79 nM, respectively, obtained by saturation binding assays. Non-specific binding for adenosine A$_{2A}$R and A$_1$R were determined in the presence of 50 μM NECA and 50 μM CPA,

respectively. Assays were performed in duplicates and compounds were tested thrice. Data were fitted in one site competition-binding model for IC$_{50}$ determination using the program GraphPad Prism 4.0 (GraphPad Software, Inc., San Diego, CA) and K_i values were calculated using Cheng and Prusoff formula.[35]

4.7. Functional assay

In the functional assay, cAMP concentrations were determined using direct cAMP EIA kit (Assay designs, USA) in treated (compounds **24–26**) HEK293 cells (stably transfected with cDNA encoding human A$_{2A}$R). Cells (1×10^6) were treated with 100 nM of compounds (**24–26**), 100 nM SCH58261 and 100 nM of NECA for 24 h, 0.1 N HCl was added to release endogenous cAMP, centrifuged at 1000g for 5 min at 4 °C. cAMP concentrations were measured,[36] and the results were compared with untreated cells (representing basal level of cAMP).

4.8. Animals

Adult Swiss Albino male mice (4–6 weeks, 20–30 g) were procured from National Institute of Communicable Diseases, Delhi, India and were kept under controlled conditions of temperature (22 ± 1 °C), humidity (60 ± 5%), and illumination (12 h light; 12 h darkness) at the animal house, Dr. B.R. Ambedkar Centre for Biomedical Research, University of Delhi, Delhi, India. The experimental protocol met the National Guidelines on the 'Proper Care and Use of Animals in Laboratory Research' (Indian National Science Academy, New Delhi) and was approved by the Animal Ethics Committee of the department. The procedures adhered to the NIH Guidelines for the Care and Use of Laboratory Animals.

4.9. Drugs

Haloperidol and SCH58261 were purchased from Sigma Chemicals Co. (St. Louis, Mo) and Tocris, respectively, India. Double distilled filtered and deionized water (Milli-Q-system Waters, Milford, MA) was used through out the study. Haloperidol, SCH58261 and compounds **24–26** were dissolved in 1% acacia in saline. Mice were divided into seven groups of four mice each. SCH58261 (10 mg/kg) and compounds **24–26** (5, 10 and 20 mg/kg) were administered intraperitoneally (ip) to each mice of the assigned group. Saline and 1% acacia in saline were injected to two control groups. After 30minutes of pre-treatment, haloperidol (2.5 mg/kg) was injected (ip) to one group and all pre-treated groups.

4.10. Catalepsy

The inability of an animal to correct an externally imposed posture (Catalepsy score) was measured at different time intervals with both limbs on a square wooden block (3 cm high) by placing the animals on a flat horizontal surface.[37] The length of time that animals held the bar without any voluntary movement was recorded, with a cutoff time of 3 min. Catalepsy score of each mice in a group was taken to compute the mean value of the group.[38]

4.11. Akinesia

Akinesia was measured by noting the latency in seconds (s) of the animals to move all four limbs and the test was terminated if latency exceeded 180 s. Each animal was initially acclimatized for 5 min on a wooden elevated (30 cm) platform (40 × 40 cm) used for measuring akinesia in mice. Using a stopwatch, the time taken (s) by the animal to move all the four limbs was recorded.[38] This exercise was repeated five times for each animal.

4.12. Statistical analysis

The data for behavioural studies were statistically evaluated for significance employing nonparametric analysis of variance (Kruskal-Wallis test) for catalepsy and akinesia employing statistical package, Graph Pad Prism 4.0. Values of $p \leqslant 0.05$ were considered significant. Results are given as mean ± SEM values.

Acknowledgements

Supplementary data

Supplementary data associated with this article can be found, in the online version, at doi:10.1016/j.bmc.2010.02.048.

References and notes

1. Ribeiro, J. A.; Sebastiao, A. M.; De Mendonca, M. Prog. Neurobiol. 2002, 68, 377.
2. Fredholm, B. B.; IJzerman, A. P.; Jacobson, K. A.; Klotz, K. N.; Linden, J. Pharmacol. Rev. 2001, 53, 527.
3. Barrington, W. W.; Jacobson, K. A.; Hutchison, A. J.; Williams, M.; Stiles, G. L. Proc. Natl. Acad. Sci. U.S.A. 1989, 86, 6572.
4. Svenningsson, P.; LeMoine, C.; Fisone, G.; Fredholm, B. B. Prog. Neurobiol. 1999, 59, 355.
5. Sebastiao, A. M.; Ribeiro, J. A. Prog. Neurobiol. 1996, 48, 167.
6. Fuxe, K.; Marcellino, D.; Genedani, S.; Agnati, L. Mov. Disord. 2007, 22, 1990.
7. Jenner, P. Neurology 2003, 61, S32.
8. Hauser, R. A.; Schwarzschild, M. A. Drugs Aging 2005, 22, 471.
9. Aoyama, S.; Kase, H.; Borrelli, E. J. Neurosci. 2000, 20, 5848.
10. Chen, J. F.; Sonsalla, P. K.; Pedata, F.; Melani, A.; Domenici, M. R.; Popoli, P.; Geiger, J.; Lopes, L. V.; Mendonça, A. Prog. Neurobiol. 2007, 83, 310.
11. Shiozaki, S.; Ichikawa, S.; Nakamura, J.; Kitamura, S.; Yamada, K.; Kuwana, Y. Psychopharmacol. 1999, 147, 90.
12. Caulkett, P. W. R.; Jones, G.; McPartlin, M.; Renshaw, N. D.; Stewart, S. K.; Wright, B. J. Chem. Soc., Perkin Trans.1. 1995, 7, 801.
13. Baraldi, P. G.; Cacciari, B.; Spalluto, G.; Pineda de Villatoro, M. J.; Zocchi, C.; Dionisotti, S.; Ongini, E. J. Med. Chem. 1996, 39, 1164.
14. Zocchi, C.; Ongini, E.; Conti, A.; Monopoli, A.; Negretti, A.; Baraldi, P. G.; Dionisotti, S. J. Pharmacol. Exp. Ther. 1996, 276, 398.
15. Baraldi, P. G.; Cacciari, B.; Romagnoli, R.; Spalluto, G.; Monopoli, A.; Ongini, E.; Varani, K.; Borea, P. A. J. Med. Chem. 2002, 45, 115.
16. http://www.kyowa-kirin.co.jp/english/news/2009/e20090115_01.html.
17. Kisselgof, E.; Tulshian, D. B.; Arik, L.; Zhang, H.; Fawzi, A. Bioorg. Med. Chem. Lett. 2005, 15, 2119.
18. Hirota, T.; Sasaki, K.; Tashima, Y.; Nakayaama, T. J. Heterocycl. Chem. 1991, 28, 263.
19. Nagamatsu, T.; Kinoshita, K.; Sasaki, K.; Nakayama, T.; Hirota, T. J. Heterocycl. Chem. 1991, 28, 513.
20. Hirota, T.; Leno, K.; Sasaki, K. J. Heterocycl. Chem. 1986, 23, 1685.
21. Jacobson, M. A. Drug Dev. Res. 1996, 37, 131.
22. Andrew, G. C.; Tara, M. S.; Laura, L. R.; Axel, M.; Lawrence, W. D.; Wenguang, Z.; Ian, H. Bioorg. Med. Chem. Lett. 2009, 19, 378.
23. Wei, J.; Wang, S.; Gao, S.; Dai, X.; Gao, Q. J. Chem. Inf. Model. 2007, 47, 613.
24. Jaakola, V. P.; Griffith, M. T.; Hanson, M. A.; Cherezov, V.; Chien, E. Y. T.; Lane, J. R.; Ijzerman, A. P.; Stevens, R. C. Science 2008, 322, 1211.
25. Catia, L.; Ippolito, A.; Michela, B.; Diego, D. B.; Dhuldeo, D. K.; Rosaria, V.; Karl, N. K.; Gloria, C. Bioorg. Med. Chem. 2009, 17, 2812.
26. William, T.; John, F.; David, U. Curr. Opin. Biotechnol. 2005, 16, 655.
27. Jiang, F. C.; Rosario, M.; Francesco, I.; David, K. G.; Beatriz, C.; Marcelo, R.; Mark, A. B.; Elizabeth, H.; Stephen Fink, J.; Malcolm, J. L.; Ennio, O.; Michael, A. S. Proc. Natl. Acad. Sci. U.S.A. 2001, 98, 1970.
28. Luthra, P. M.; Prakash, A.; Barodia, S. K.; Kumari, R.; Mishra, C. B.; Kumar, J. B. Neurosci. Lett. 2009, 463, 215.
29. Varty, G. B.; Hodgson, R. A.; Pond, A. J.; Grzelak, M. E.; Parker, E. M.; Hunter, J. C. Psychopharmacology 2008, 200, 393.
30. Luthra, P. M.; Mishra, C. B.; Jha, P. K.; Barodia, S. K. Bioorg. Med. Chem. Lett. 2010, 20, 1214.
31. Shaker, R. M. ARKIVOC 2006, XIV, 68.
32. Morris, G. M.; Goodsell, D. S.; Halliday, R. S.; Huey, R.; Hart, W. E.; Belew, K. R.; Olson, A. J. J. Comput. Chem. 1998, 19, 1639.
33. Accelrys Inc., ForceField-Based Simulations. San Diego: Accelrys, Inc., 2002. URL http://www.accelrys.com/doc/life/insight2000.1/ffbs/FF_SimulTOC.html.
34. Discover 3 User Guide, San Diego: MSI, USA, 1999.
35. Cheng, Y.; Prusoff, W. H. Biochem. Pharmacol. 1973, 22, 3099.
36. Tijssen, P. Practice and Theory of Enzyme Immunoassays; Elsevier: Amsterdam, 1985.
37. Costall, B.; Naylor, R. J. Eur. J. Pharmacol. 1974, 27, 46.
38. Luthra, P. M.; Barodia, S. K.; Raghubir, R. J. Neurosci. Methods 2009, 178, 284.